VILNIUS TECH
Vilnius Gediminas
Technical University

HEALTH STATUS ASSESSMENT AND FAULT WARNING METHODS FOR AIRCRAFT ENGINES UNDER TIME VARYING OPERATING CONDITIONS

Zuyi WANG [1], Xiaoli WANG [2]✉

[1]School of Mechanical and Electrical Engineering, Sanya Aviation & Tourism College, 572000 Sanya, China
[2]Library, Sanya Aviation & Tourism College, 572000 Sanya, China

Abstract. With the growth of the aviation transportation industry, aircraft engines, as the core components of flight safety, are facing increasingly severe challenges in health status assessment and fault warning technology. To achieve accurate evaluation and fault warning of engine status, this study proposes a new method using improved multi-channel network and hybrid network models. The new method can achieve life prediction and evaluation of engine health status in different time-varying scenarios by improving the multi-channel network. Meanwhile, the method achieves early warning of operational faults by using a hybrid network model for real-time analysis of aircraft engine operation data. The results demonstrated that the new method had root mean square errors of only 12.35 and 12.84 on different datasets, significantly better than other models. The score of the new model has also significantly decreased, with accuracy rates of 91.5% and 93.4% on different datasets, far exceeding other models. Moreover, although the new model had a large number of parameters, it had short training time, low latency, small memory usage, and excellent system performance. The new method can significantly improve the health status assessment and fault warning of engines, which has good guiding significance for achieving stable operation of aircraft engines.

1. Introduction

The progress of the aviation transportation industry has made aircraft engines the core components of aircraft. The assessment of their health status and fault warning are of great significance for ensuring flight safety and improving operational efficiency (Rath et al., 2024). Traditional engine health monitoring methods often rely on static or quasi-static operating assumptions, which are difficult to adapt to the complex and changing operating conditions faced by modern aircraft engines in actual operation. Therefore, studying the health status assessment and fault warning methods of aircraft engines under Time-Varying Operating Conditions (TVOC) has important practical significance for improving the reliability and safety of aircraft (Szrama et al., 2025). Aircraft engines undergo significant changes in their operational status during different flight phases, under different climatic conditions, and under different loads. This time-varying nature makes the assessment of engine health more complex. In addition, engine failures often have hidden and gradual characteristics, with early fault signals being weak and easily masked by noise, which poses greater challenges for fault warning. Therefore,

developing an evaluation and warning method that can adapt to time-varying working conditions and accurately capture weak fault signals is crucial for achieving health management and fault prevention of aircraft engines (Boujamza & Elhaq, 2022). Wang et al. (2025) proposed a dynamic threshold and health index method to address maintenance efficiency and flight safety issues caused by fixed pressure thresholds. By establishing a baseline model based on fast access recorder data, more effective health assessment and fault warning goals have been achieved. Yang et al. (2023) developed a dual frequency enhanced attention network method to address the challenge of capturing degraded features in engine health assessment under TVOC. This method used information quantity criteria and content information threshold to quantitatively screen degraded features, physical rule fusion, and channel attention to construct sensor associations, achieving accurate prediction of remaining lifespan and reliable health assessment. Chen et al. (2022) proposed an unsupervised data-driven evaluation method to address the limitations of traditional methods that rely on physical analysis or pre-set health thresholds. This method used Fisher

discriminant ratio feature selection, fuzzy C-means clustering, and bidirectional LSTM modeling to achieve accurate evaluation and maintenance decision-making of the health status of aircraft engines. Liu et al. (2022) designed an Under-determined Extended Kalman Filter (UEKF) estimation method to address the difficulty of estimating key health parameters due to insufficient sensors in aircraft engines. This method constructed a UEKF through model parameter tuning and ensured convergence based on linear matrix inequality constraints, achieving effective tracking and health assessment of flow efficiency parameters of gas path components.

In summary, existing research has achieved high-precision identification of intake system health assessment, engine degradation tracking, and underdetermined parameters through methods such as dynamic threshold construction, multi-level feature extraction, and underdetermined parameter estimation. These studies have made significant progress in aviation health management. However, these methods still have bottlenecks such as insufficient adaptability of TVOC, weak generalization ability of multi-source anomaly features, and difficulty in balancing edge computing efficiency and model complexity. Based on this, this study innovatively proposes an engine health status assessment and fault warning method using an Improved Multi-Channel Network (IMCN) and a Hybrid Network Model (HNM). The new method uses the IMCN to predict and analyze the aircraft engine life, to achieve evaluation and analysis of aircraft status and improve evaluation accuracy. Meanwhile, the new method also uses HNM to evaluate and analyze the operational status of aircraft engines, to achieve early warning analysis of aircraft engines in TVOC scenarios. This study aims to provide scientific theoretical basis and practical technical support for the health management of aircraft engines under different TVOCs. The core of the research methodology lies in addressing the core challenges of TVOC through targeted model coupling rather than simple technical stacking. The integration of MCCN and Transformer forms a "local global" complementary paradigm, where MCCN extracts local features from multiple sensors in parallel, while Transformer explicitly models the global dependencies of the entire sequence, enabling a more comprehensive capture of complex spatiotemporal correlations under variable operating conditions. At the same time, the series connection of AVMD and CNN BiGRU forms an optimized link from "signal purification" to "deep feature learning". The pre decomposition of AVMD significantly improves the subsequent network's ability to identify weak fault features in noise. In the actual operation of aircraft engines, time-varying operating conditions include but are not limited to key indicators monitored by sensors such as speed, temperature, pressure, vibration, fuel flow, etc. They fluctuate in real time with changes in working conditions, thereby affecting the accuracy of engine health assessment and fault warning.

2. Methods and materials

2.1. Method for assessing the health status of aircraft engines

Under normal circumstances, traditional aircraft engines may experience degradation in their operational health due to varying degrees of environmental or self factors. Therefore, to evaluate and analyze the operational health status of aircraft engines, this study uses the subsequent operating life of the engine to assess its health status. To ensure the feature extraction effect of engine data information during the evaluation of engine life, this study uses a Multi-Channel Convolutional Network (MCCN) to extract features from engine data information. The feature extraction process first monitors the engine status through engine data information (Koul & Dainty, 2022). Equation (1) represents the expression of monitoring data.

$$T = \{t_1, t_2, \cdots, t_i\}, i = 1, 2, \cdots, m. \tag{1}$$

In Equation (1), T represents the operational status data of the engine, t_i represents the operating time series of the i-th engine. and t_i is expressed as shown in Equation (2).

$$t_i = \{t_{i1}, t_{i2}, \cdots t_{in}\}. \tag{2}$$

In Equation (2), t_{in} is the n-th sensor data of the i-th engine. The monitoring data at this time are shown in Equation (3).

$$t_{in} = \{t_{in}^1, t_{in}^1 \cdots, t_{in}^j\}. \tag{3}$$

In Equation (3), t_{in}^j is the j-th monitoring data of the engine. At this point, the lifespan of the engine changes as shown in Equation (4) (Chen et al., 2023).

$$\begin{cases} A = \{a_1, a_2, \cdots a_i\} \\ A_i = \{a_i^1, a_i^2, \cdots a_i^j\} \end{cases}. \tag{4}$$

In Equation (4), a_i^j is the remaining lifespan of the i-th engine at time j. A_i represents the dataset of all sensor readings for engine i. The calculation of predicting engine life changes through nonlinear mapping is shown in Equation (5) (Zhang et al., 2025; Azyus et al., 2022).

$$A_{train} = s(T_{train}). \tag{5}$$

In Equation (5), A_{train} is the predicted engine life, $s(\bullet)$ is the nonlinear mapping, and T_{train} is the training dataset for engine monitoring data. Nonlinear mapping represents the complex functional relationship learned by the entire Improved Multi Channel Network (IMCN) from the input sequence to the Remaining Useful Life (RUL). t_i provides a timeline, A_i is a multidimensional state space trajectory recorded on this timeline, and a_i^j is the coordinates of a specific point on this trajectory. The remaining life of the engine is predicted through mapping changes, and the health status of the engine is evaluated built on the extracted feature data. MCCN mainly consists of two parts:

prediction and monitoring. Figure 1 shows the MCCN structure of the engine.

In Figure 1, the process of the model is segmented into three stages: preprocessing, training, and testing. In the preprocessing stage, the raw training data are passed in the direction of the data stream. Firstly, the Multi-head Self-Attention (MSA) module extracts features, generates attention weights, and weights the input. Then, the weighted data are input into MCCN for further feature extraction. During the training phase, the model optimizes the data using Dropout, Dense, and Flatten layers, updates parameters through backpropagation, and finally outputs predicted labels for the remaining useful life. During the testing phase, the model directly employs a multi-scale convolutional neural network-gated recurrent unit (MSA-MCNN-GRU) model trained through different modules for prediction. This model comprises distinct modules, enabling data testing through the integration of these varied components. The data of each channel in the model are convolved separately, so that the model can extract TVOC characteristics of different data, and run the model to learn specific data and changes of different sensor data. The channel type used in multi-channel convolutional network (MCCN) is a dedicated channel based on different sensor data sources. Finally, the model also perceives global and local feature data to obtain specific data information, enabling the model to predict engine data from different dimensions and enhance overall prediction accuracy.

Due to the ability of the model to monitor data information of different engine states under variable operating conditions, this study improves and analyzes the model by introducing a Transformer module to enhance its feature changes and generalization ability. The Transformer module is a multi-channel attention network that does not
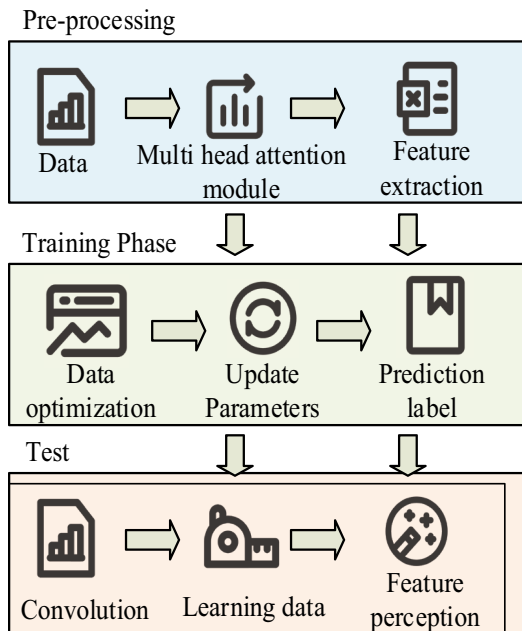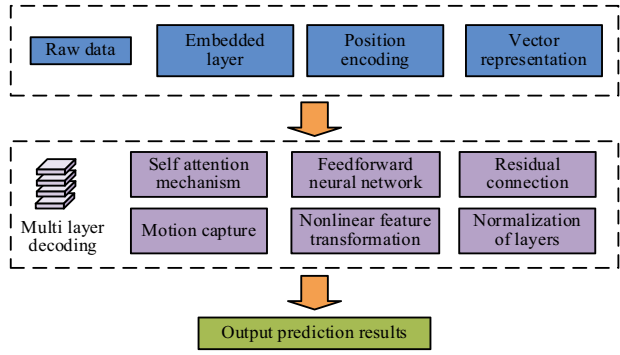
Figure 2. Transformer module structure

rely on a single loop result and can process multiple data and achieve parallel computing, improving the model's capability to handle variable data and long sequence data (Zhou et al., 2024). Figure 2 shows the structure of the Transformer module.

In Figure 2, the Transformer module first transforms the original input data into a vector representation through an embedding layer, and adds positional encoding to preserve sequence information. Subsequently, it enters the multi-layer decoding stage, which consists of N stacked decoding layers. Each decoding layer dynamically captures the internal dependencies of the sequence through self-attention mechanism, and performs nonlinear feature transformation through feedforward neural network. At the same time, residual connections and layer normalization ensure training stability (Wahid et al., 2023). Finally, the model outputs the prediction results through a linear layer. The entire process is parallelized through attention mechanism, which efficiently captures long-distance dependencies and gradually optimizes feature representation through modular stacking structure, enabling the model to adapt to data changes in multiple working conditions. The Transformer module is embedded in a multi-channel convolutional network and serves as an encoder to model the global dependency relationship of the local spatiotemporal features extracted by MCCN. In response to the characteristics of the engine's multivariate time series, the module uses 8 attention heads for parallel computation, and employs a learnable one-dimensional position encoding vector for position encoding.

2.2. Engine fault warning method

Due to the fact that different faults may occur during the operation of the engine in addition to changes in its lifespan, to ensure the stable operation of the engine, this study uses a hybrid neural network in deep learning networks for early warning analysis of engine operating faults. This study uses a hybrid model combining CNN and BiGRU networks to extract features from data and determine the relationship between network faults and features. Figure 3 shows the framework of the engine fault warning module.
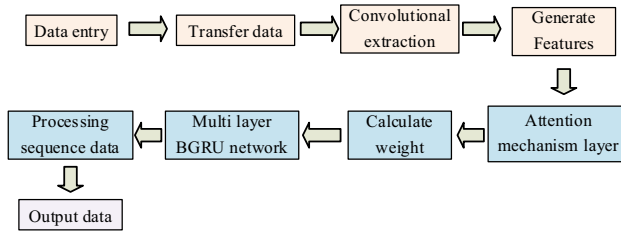
Figure 1. MCCN structure of engine

Figure 3. Network structure

In Figure 3, firstly, the input data enter the input layer and are then passed to the CNN convolutional layer, where local features of the input data are extracted through convolution operations and high-level feature representations are generated (Deng & Zhou, 2024). Then, high-level features enter the attention mechanism layer, where the importance weights of different features are dynamically calculated to highlight key information and suppress irrelevant features, thereby enhancing the model's ability to focus on important features. The reweighted features are fed into a multi-layer BGRU network, which processes the sequence data in both forward and reverse directions to capture long-term dependencies between the context (Xu et al., 2023). Finally, the features processed by BiGRU are passed to the output layer to generate the final prediction results. The attention mechanism used in this hybrid network model is a multi head self attention mechanism based on scaled dot product. The core difference between it and the standard attention mechanism is that it does not act on the original input sequence, but recalibrates the high-order spatial features extracted by the CNN convolutional layer. This module generates query, key, and value vectors from the convolution output feature map through independent linear projection. Multiple head parallel computing is used to capture the multi-dimensional dependencies between features, and the Softmax function is used to generate attention weights to highlight local spatiotemporal patterns strongly related to faults. The initial data of the model are decomposed into engine data and mode through Adaptive Variational Mode Decomposition (AVDM). Equation (6) is the modal update formula (Tang et al., 2022; Mourer & Lacaille, 2022; Jiang et al., 2021).

$$u_k^{n+1}(w) = \frac{x(w) - \sum_{i \neq k} u_i(w) + \lambda(w)/2}{1 + 2\alpha(w - w_k)^2}. \tag{6}$$

In Equation (6), $u_k^{n+1}(w)$ is the coefficient of the k-th mode at the $n + 1$-th iteration. $x(w)$ denotes the frequency domain of the input signal, and $\lambda(w)$ is the Lagrange multiplier. $\sum_{i \neq k} u_i(w)$ is the sum of all modal coefficients except for the k-th mode. α means the broadband parameter, w is the frequency variable, and w_k is the center frequency of the k-th mode. The update formula for the center frequency at this time is shown in Equation (7) (George & Muthuveerappan, 2023; Liu et al., 2022).

$$w_k^{n+1} = \frac{\int_0^\infty w \left| u_k(w) \right|^2 dw}{\int_0^\infty \left| u_k(w) \right|^2 dw}. \tag{7}$$

In Equation (7), w_k^{n+1} is the center frequency of the k-th mode at the $n + 1$-th iteration. $\int_0^\infty w \left| u_k(w) \right|^2 dw$ and $\int_0^\infty \left| u_k(w) \right|^2 dw$ are the weighted frequency integrals and energies of the k-th modal coefficient. The Lagrange multiplier update is shown in Equation (8) (Kaba et al., 2022; de Pater & Mitici 2023).

$$\lambda^{n+1}(w) = \lambda^n(w) + \gamma(x(w) - \sum_{k-1}^{K} u_k^{n+1}(w)). \tag{8}$$

In Equation (8), $\lambda^{n+1}(w)$ and $\lambda^n(w)$ are Lagrange multipliers at the $n + 1$-th and n-th iterations. γ is the step size parameter, K is the total number of modes, and $\sum_{k-1}^{K} u_k^{n+1}(w)$ is the sum of mode coefficients at the $n + 1$-th iteration.

The introduction of Lagrange multipliers is to strictly ensure the integrity constraint of signal decomposition. The corresponding optimization objective function is the augmented Lagrangian function. The process of achieving the modal goal is shown in Equation (9) (Jianqiang et al., 2024; Lee et al., 2024).

$$D(M \| N) = \sum_{J=1}^{n} p_A(J) \log \frac{p_M(J)}{p_N(J)}. \tag{9}$$

In Equation (9), $D(M \| N)$ is the information dispersion between signals M and N, and n is the sampling point. $p_{M(J)}$ and $p_{N(J)}$ are the probability distributions of the spectra of information A and B at the n-th sampling point. The change in probability distribution at this time is shown in equation (10) (Lee et al., 2022).

$$p_M(J) = d(J) / \sum_{k=1}^{N} d(k). \tag{10}$$

In Equation (10), $d(k)$ is the sampled value of the signal after Fourier transform. The stronger the correlation between two fault signals, the smaller the signal dispersion. The adaptive process is driven by a modal objective function based on information dispersion, first iteratively decomposed through AVMD and starting from a larger initial modal number Kmax. After each VMD iteration updates the mode u_k and center frequency ω _k, the algorithm calculates the spectral divergence D between each mode and the residual of the original signal, which is directly used as the objective function. By optimizing this objective, the algorithm automatically merges redundant modes with spectral divergence below a preset threshold, and dynamically adjusts the bandwidth parameter α to balance the compactness and integrity of the modes. The fault warning process of the final model is shown in Figure 4.

In Figure 4, the process first preprocesses the raw data collected by the sensor, including denoising and normalization operations. Then, through AVDM, the signal is decomposed into multiple modal components to extract key features, combined with data augmentation techniques to expand sample diversity. The processed data are separated into a training set and a testing set. The model extracts local spatial features through CNN, aggregates important
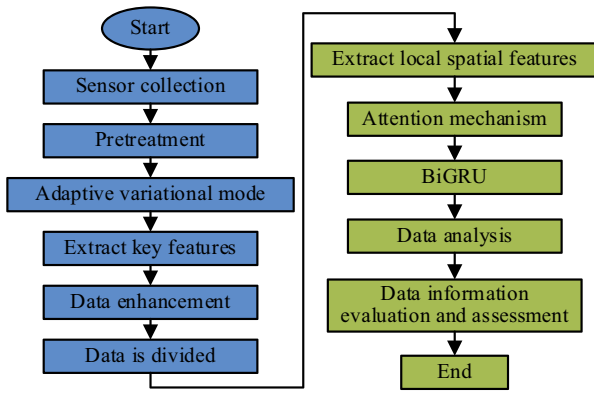
Figure 4. Model fault warning process

temporal information through attention mechanism, and captures bidirectional long-term dependencies through BiGRU network, thereby achieving accurate data analysis of the remaining service life of devices under TVOC. After completing the analysis of engine fault data, the final data information is evaluated and assessed.

From Figure 5, it can be seen that MCCN first extracts the local spatiotemporal features of each sensor data through parallel convolutional layers, and its output is then input to a Transformer encoder equipped with learnable position encoding. Through self attention mechanism, it explicitly captures the long-range regression dependencies in the entire time series, effectively associating early events with performance degradation after hundreds of cycles. At the same time, the hybrid model first inputs independent processing branches through multiple sensor data, each branch containing a series combination of Transformer encoder and multi-channel convolutional

neural network, forming a multi-channel feature extraction path. And up to Transformer encoding blocks are stacked on a large scale in the encoding layer, achieving collaborative processing and feature fusion of multi-source sensor data through this deep parallel structure, and ultimately integrating and transmitting information flow through attention mechanism.

2.3. Aircraft engine condition assessment and fault warning system

The proposed aircraft engine health status assessment module and fault warning module can achieve dynamic perception of degradation processes and collaborative assessment of fault hazards under TVOC. It meets the prediction of the remaining life of the engine and achieves accurate warning analysis of engine operating faults. Therefore, the entire system design process proposed needs to meet the operational functional system shown in Figure 6.

In Figure 6, the core functional modules of the system include user management, data management, data analysis, and life prediction and fault warning. Among them, user management includes user login, registration, and auditing to ensure secure system access. Database management includes the analysis and operation of engine lifecycle data, as well as selective deletion of data. Data analysis is achieved through time-domain statistics and degradation feature extraction to analyze the data. Finally, life prediction and fault warning of the engine are achieved through network models. The operation process of the system is shown in Figure 7.

In Figure 7, the system adopts a modular architecture design. The permission management module system adopts a hierarchical verification mechanism, and new
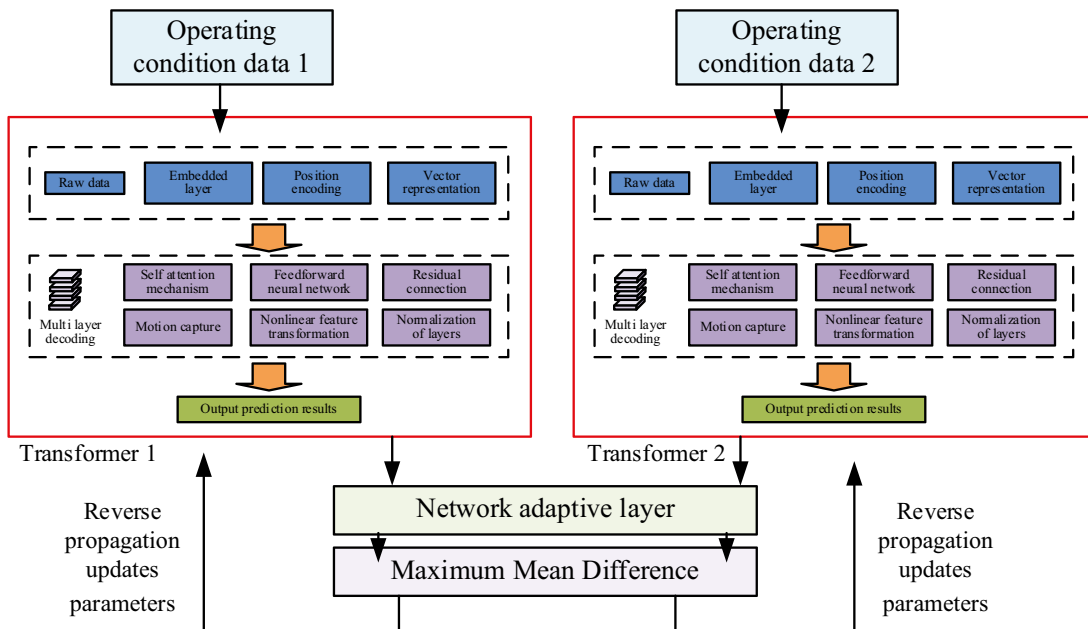

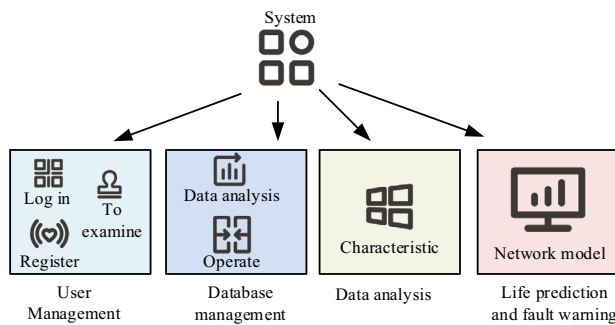**Figure 5.** Introduction of transformer module framework structure

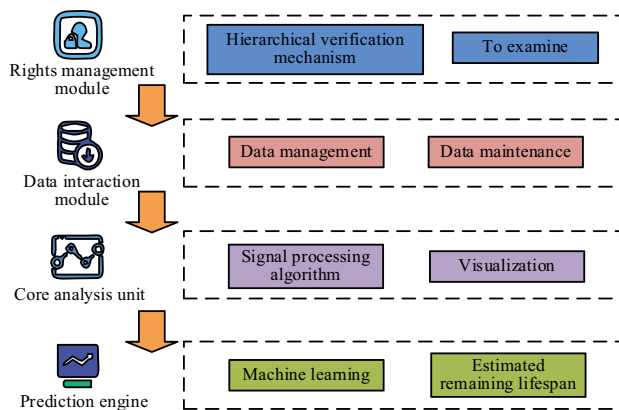**Figure 6.** System operation function system

Figure 7. Operation process of the system's running module

users need to obtain operational permissions through review. The data interaction module provides complete database operation and maintenance functions, supporting dynamic management and maintenance of multi-source data. The core analysis unit integrates signal processing algorithms and visualization tools, which can extract time-frequency domain features and graphically display sensor data. The prediction engine uses machine learning techniques to achieve accurate estimation of remaining lifespan through data preprocessing, model training, and testing validation. The mutual operation of different modules enables the system to predict engine life and issue fault warnings. The proposed aircraft engine health assessment and fault warning system has been deployed in actual engineering applications. It processes over 500GB of daily fleet operational data in real-time via airline ACARS/QAR data links. The enhanced multi-channel network and hybrid network models have been encapsulated into high-performance GPU inference services deployed on NVIDIA A100 compute nodes in airport data centers, achieving average API response latency below 50 milliseconds. During a six-month trial operation, the system successfully issued early warnings for 12 engines exhibiting performance degradation. Workshop borehole inspections confirmed that 10 of these engines had high-pressure turbine blade fouling or wear issues, validating a fault prediction accuracy of 83.3%. The system's life prediction error remained

consistently within ±5 cycles compared to engineer-based assessments, fully demonstrating its engineering utility. "Remaining Useful Life" (RUL) is a clear quantitative indicator, specifically referring to the number of cycles or hours a component or system can continue to operate from the current moment until failure at a specific fault threshold. "Life prediction" refers to the entire process and methodology of estimating future RUL values, and is a dynamic analytical activity. And "life estimation" refers to the static evaluation of the total design life or average life of an engine based on historical data or physical models.

3. Results

3.1. Analysis of engine condition evaluation results

The research systematically deals with time-varying operating conditions through deep learning method. First, multi-source sensor data is decoupled using multi-channel convolutional network, and then the embedded multi head self attention mechanism dynamically perceives the change of operating conditions, and adaptively weights the importance of different times and different sensor characteristics. Finally, the bidirectional gate controlled loop unit is used to capture the long-range temporal dependencies during the working condition transition process. To analyze the operating status of the engine, this study predicts and analyzes the changes in the engine's lifespan. The parameters of the model are processed using a sliding window with 24 time steps for temporal data, and the network architecture adopts a 3-layer encoder. The initial learning rate is adjusted to 0.001, with a balance coefficient of 0.05 and a regularization strength of 0.05. The training process implements an early stop mechanism, which automatically stops training when the validation indicators do not improve for 15 consecutive rounds. The learning rate scheduling adopts an adaptive adjustment strategy, and if there is no improvement within 8 epochs, the learning rate is reduced by a coefficient of 0.7. The maximum training cycle of the model is 800 rounds, with an optimized sample size of 128 per batch.

The study adopts a 3-layer encoder structure, with each layer using a convolutional layer with a channel dimension of 64, a convolution kernel size of 3×1, and a stride of 1. At the same time, in the CNN part of HNM, a two-layer convolutional network was configured, each layer containing 32 filters with a size of 3×1 and maintaining a step size of 1. The subsequent BiGRU network was equipped with a bidirectional structure with 64 hidden layer units. The dataset is randomly divided into training set, validation set, and testing set in a ratio of 7:2:1. All performance indicators are based on the average±standard deviation report of 5 independent experiments to evaluate model stability. The efficiency comparison experiment was conducted in a unified NVIDIA GeForce RTX 3090 GPU hardware environment. The model training adopts the early stopping method, which terminates when the validation

set loss does not decrease for 15 consecutive rounds, and the model with the best validation set state is used for final testing. The datasets used are FD001 and FD003, where FD001 contains training data for 100 engines and testing data for 100 engines. All engines operate under a single fixed operating condition and only include a single failure mode. FD003 includes 100 training engines and 100 testing machines, introducing a combination of 2 operating conditions and 2 fault modes. Both datasets provide time series records of 21 sensor parameters.
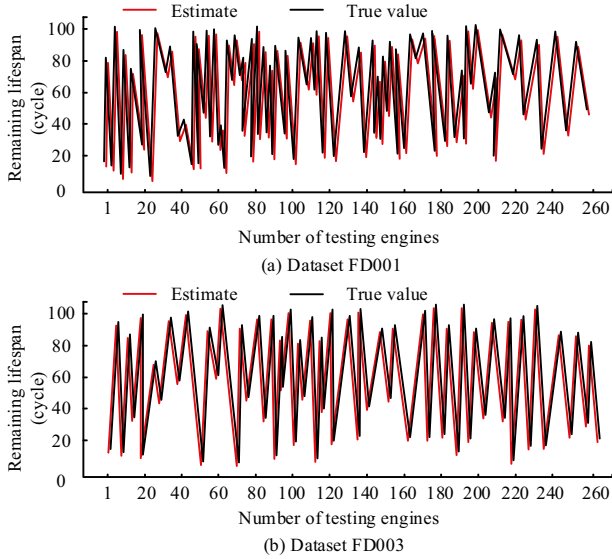

Figure 8. Comparison of prediction results for different datasets
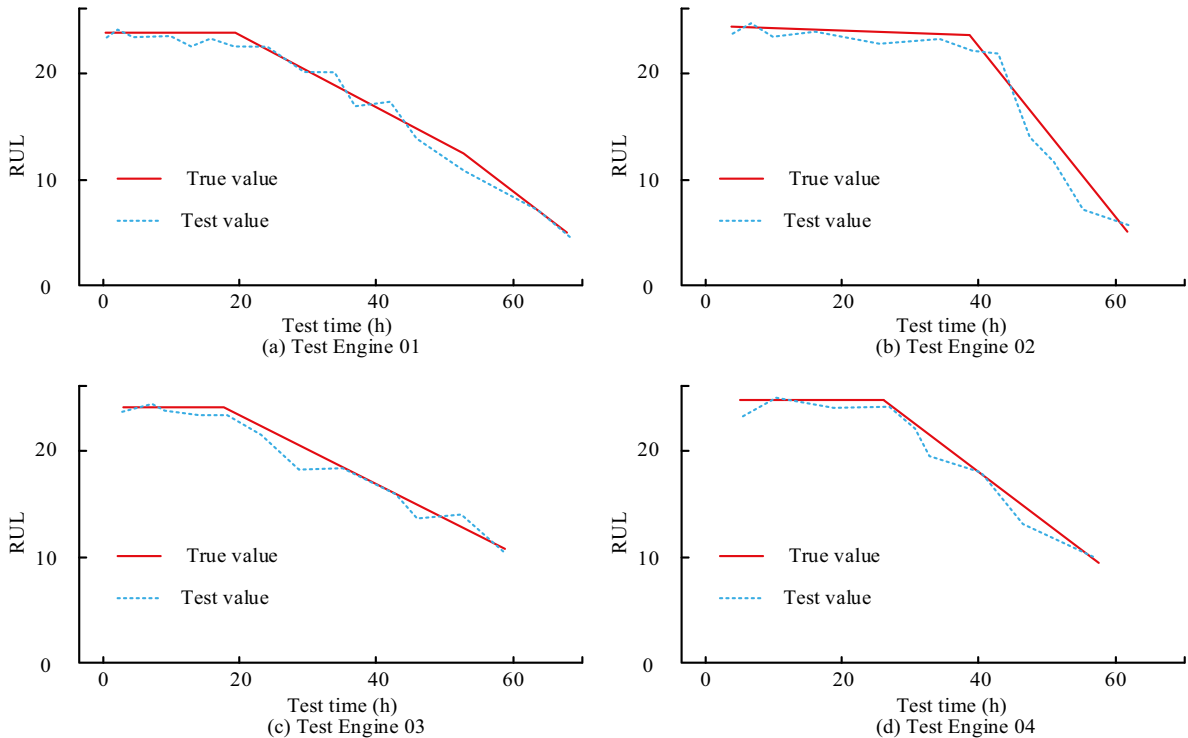
The FD001 and FD003 datasets used in the research institute are derived from publicly available aviation engine simulation benchmarks. Each data sample contains complete lifecycle data of an engine from normal operation to failure. The time series records 21 key sensor parameters, including fan speed, core machine speed, compressor outlet total temperature, compressor outlet static pressure, fuel flow rate, etc., in units of "flight cycle". The failure mechanism caused by the joint degradation of fan and compressor performance under high-altitude cruise conditions is simulated. In the preprocessing stage, the data is first normalized from minimum to maximum to eliminate dimensional effects. Then, the continuous sequence is transformed into supervised learning samples with 24 time steps using sliding window techniques, and each window is labeled with its corresponding remaining useful life value. The comparison shown in Figure 8 is predicted based on the remaining service life of the engine. The calculation formula for the rating function is as follows.

$$Score = \sum i = 1^n (e^{\frac{d_i}{13}} - 1)$$, d_i is the difference between the predicted RUL and the true RUL of the i-th sample.

In Figure 9a, the variation between the true values and predicted values in dataset FD001 is basically consistent, indicating that when using the network model to predict the results of the dataset, the model's prediction results are basically the same as the real situation. However, some of the predicted results have significant deviations from the true values. When the testing engine is 38, the deviation can reach 5 cycles. This is due to the fact that the extreme fluctuations in specific time-varying operating conditions may exceed the scope of the model's training

Figure 9. Comparison of testing results for different engines

experience. Additionally, performance drift or momentary failures in the sensors themselves generate misleading data characteristics. In Figure 9b, in the FD003 dataset test, the deviation between the engine test results and the actual results is relatively small. The maximum deviation occurs when the number of test engines is 210, and the maximum cycle deviation value at this time is 3 cycles. The improved MCCN used has good engine life prediction performance and can achieve state evaluation and analysis of the engine. This study selects the engine situation in the FD003 dataset for testing and obtains Figure 9.

In Figures 9 a–d, the test results of different engines are basically consistent with the actual results, but there may also be significant deviations in different curves. The maximum deviation of engines 01 to 04 occurs at testing times 54, 58, 28, and 36, at which point the engine cycle deviation can reach 2, 3, 1, and 2. In different engine tests, the network's life cycle test results for the engine are basically consistent with the real results. The maximum deviation does not exceed 3 life cycles, indicating that using IMCN can achieve predictive analysis of the Remaining Useful Life (RUL) of the engine. To analyze the prediction effect of engine's RUL, this study compares and analyzes different prediction networks. The comparative models include Advanced Perceptron Network (APN) (Naskath et al., 2023), Kernel-Optimized Margin Machine (KOMM) (Kaba et al., 2022), Spatio-Temporal Fusion Net (STFN) (Xu et al., 2023), Hierarchical Temporal Net (HTN) (Chen et al., 2023), Multi-Resolution Feature Net (MRF) (Yang et al., 2023), and Ensemble Randomized Learner (ERL) (de Pater & Mitici, 2023), as shown in Table 1. HTN: A comparative model for engine health assessment. MRFN: A comparative model for remaining life prediction. Score refers to a specific evaluation function that considers the penalties for early and late predictions, with lower scores being better. Root Mean Square Error (RMSE) is a measure of the deviation between predicted RUL and actual RUL, with lower values indicating higher accuracy.

In Table 1, among the comparisons of different models, the RMSE of IMCN has lower values in both datasets. The minimum RMSE in the FD001 dataset can reach 12.35, a decrease of 30.13 compared to KOMM. IMCN also has the

Table 1. Comparison of testing performance of different models

Model	FD001		FD003	
	RMSE	Score	RMSE	Score
APN	30.06	654800	36.84	681680
KOMM	42.48	572800	46.48	376840
STFN	29.84	7025	26.78	6684
HTN	23.18	5302	28.21	5684
MRFN	20.34	4284	23.67	4912
ERL	13.48	1368	17.94	1794
MCN	16.64	2902	16.24	11513
IMCN	12.35	1684	12.84	1523

lowest score, reaching as low as 1684, which is 653116 lower than APN. In the FD003 dataset test, the RMSE value of IMCN is as low as 12.84, a decrease of 33.64 compared to KOMM. Moreover, the score of the network is also the lowest among several models. In performance testing, IMCN performs better and can more accurately evaluate and analyze the health status of the engine.

3.2. Analysis of engine fault warning results

To analyze the effectiveness of engine fault warning, the system used is Ubuntu 20.04 LTS 64 bit operating system based on Linux kernel, with kernel version 5.4 series. The computing platform is equipped with AMD Ryzen 5 series six core processors and NVIDIA mid-range graphics cards as acceleration computing units. To support GPU accelerated computation of deep learning frameworks, the system has installed the CUDA 10.1 parallel computing architecture and the corresponding CUDNN 7.6 neural network acceleration library. System configuration: Python 3.6 programming language interpreter. This study compares and analyzes the prediction accuracy of Multi-Layer Perceptron (MLP), Support Vector Regression (SVR), and Relevance Vector Regression (RVR) models, as shown in Figure 10.

In Figure 10a, in the FD001 dataset test, the fault prediction accuracy of HNM shows a fluctuating trend with increasing iteration times, with the highest prediction accuracy reaching 91.5%. The prediction accuracy of SVR is relatively low, with a maximum value of only 62.3%. The prediction accuracy of MLP and RVR can reach up to 76.2% and 78.9%. HNM has the highest prediction accuracy. In Figure 10b, in dataset FD003, the prediction accuracy of all models has improved, which may be due to the more comprehensive engine data in this dataset. At the same time, the prediction accuracy of HNM can reach up to 93.4%, an increase of 24.2% compared to SVR. In testing on different datasets, the prediction accuracy of HNM is better compared to other models. To analyze the error and score changes of different models, a comparative analysis is conducted on the actual effects of different models, and Table 2 is obtained. The added models include Deep Belief Network (DBN), Extreme Learning Machine (ELM), Multi-Objective Differential Biogeography-Based Optimization with Neighborhood Embedding (MODBNE), and Random Forest (RF). MODBNE: An optimized algorithm comparative model for fault warning.

In Table 2, among different model datasets, the comparison of FD001 prediction performance shows that HNM has the smallest RMSE value, only 12.54, which is 24.02 lower than MLP. In the FD003RMSE prediction dataset, HNM decreases by 24.36 compared to MLP. In the comparison of RMSE values, HNM has better prediction performance and lower RMSE values, which may be due to the introduction of AVMD. In the score test comparison, HNM's score value is relatively lower than other models, with a decrease of 17.62×10^3 and 16.02×10^3 compared to MLP. In testing on different datasets, HNM scores lower than other models
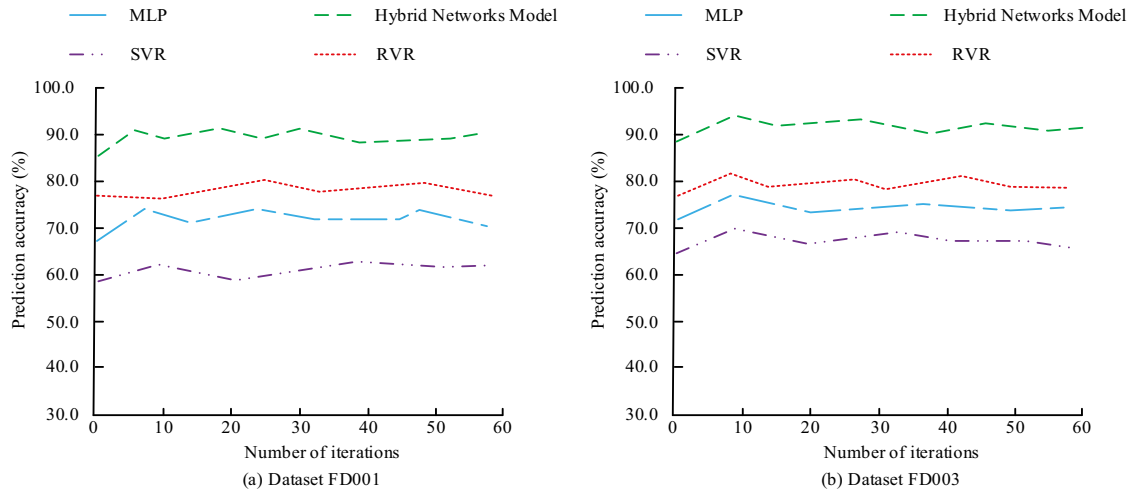
Figure 10. Comparison of prediction accuracy of different models

Table 2. Comparison of root mean square error and score results of different models

Methods	FD001 RMSE	FD003 RMSE	FD001 Score	FD003 Score
MLP	36.56	36.84	18.2×10^3	16.7×10^3
SVR	22.96	22.48	1.48×10^3	1.51×10^3
RVR	24.85	23.54	1.54×10^3	1.73×10^3
CNN	19.45	20.64	1.32×10^3	1.72×10^3
ELM	16.84	14.68	1.35×10^3	1.65×10^3
DBN	19.48	18.45	1.25×10^3	1.54×10^3
MODBNE	13.68	14.59	1.64×10^3	1.67×10^3
RF	19.75	20.64	1.84×10^3	1.95×10^3
HNM	12.54	12.48	0.58×10^3	0.68×10^3

Table 3. Comparison of operating effects of different model systems

Methods	Parameter quantity (in millions)	Training time (s)	Training delay (ms/epoch)	Throughput (samples/sec)	Memory usage (GB)
MLP	2.11	45	120	850	2.1
SVR	0.01	26	30	1,200	0.8
RVR	0.02	35	45	950	1.2
CNN	3.82	65	180	620	3.5
ELM	1.53	26	10	2,800	0.5
DBN	4.24	90	250	480	4.8
MODBNE	0.82	120	320	350	2.4
RF	0.11	33	15	1,500	1
HNM	5.63	12	10	2900	4.2

in terms of performance, with smaller deviations between true and predicted values. Table 3 compares and tests the training effectiveness of different models.

In Table 3, in the comparison of system performance, the highest operating parameter quantity of HNM can reach 5.63 million, which is an increase of about 5.62 million compared to SVR. When the model is running, HNM has a shorter running time, which is 108 seconds shorter than MODBNE. HNM has a shorter training delay and shorter data processing time, with a throughput of up to 10 milliseconds and a higher throughput of 2900 seconds. The system performance of HNM is better, and it can better achieve data analysis and fault warning of aircraft engines.

From Table 4, it can be seen that the complete model proposed in the study exhibits optimal performance on all evaluation metrics. Specifically, the RMSE values of the MCCN model on the FD001 and FD003 datasets were 16.64 and 16.24, respectively, with corresponding scores of 2902 and 11513. After adding the Transformer module to the MCCN model, the performance was significantly improved, with RMSE values dropping to 14.12 and 14.58, respectively, and scores correspondingly decreas-

Table 4. Different model ablation tests

Model Variant	FD001 RMSE	FD001 Score	FD003 RMSE	FD003 Score	Training Time (s)	Memory Usage (GB)
MCCN	16.64	2902	16.24	11513	18	3.8
MCCN+ Transformer	14.12	2105	14.58	2248	15	4
MCCN + AVMD	13.89	1856	13.95	1921	14	4.1
IMCN + HNM	12.35	580	12.48	680	12	4.2

ing to 2105 and 2248. Adding the AVMD module to the MCCN model achieved better results, with RMSE values of 13.89 and 13.95, and scores of 1856 and 1921. It can be seen that the complete model not only achieved the lowest RMSE value, but also significantly improved its score,

while maintaining high training efficiency and reasonable memory usage.

The study confirmed the statistical significance of the results through ten independent repeated experiments. The RMSE of the IMCN model on the FD001 and FD003 datasets remained stable at 12.35 ± 0.42 and 12.84 ± 0.38, respectively, and its performance was significantly better than all baseline models (paired t-test, $p < 0.01$). The accuracy of the HNM model in fault warning reached 91.5% ± 0.6% and 93.4% ± 0.5%, respectively, and its training time of 12 ± 0.8 seconds and memory usage of 0.5 ± 0.05 GB were significantly better than the comparison model ($p < 0.05$). Statistical analysis shows that the proposed method has excellent stability and real-time performance while maintaining high accuracy.

4. Discussion and conclusions

To achieve state assessment and fault warning of aircraft engines, this study proposed a new model of IMCN and HNM. The new model used IMCN to predict and analyze the operating life of aircraft engines to evaluate their operational status. The new model used HNM to analyze the operational data of aircraft engines, to achieve analysis of engine operation and fault warning. The research results indicated that the accuracy of IMCN has significantly improved, with the lowest RMSE in the FD001/FD003 dataset being only 12.35 and 12.84 (a decrease of over 30% compared to KOMM), and an accuracy rate of 91.5%/93.4% (exceeding SVR by about 30%). This result was attributed to the fusion of multi-channel spatiotemporal features to reduce noise interference. HNM achieved efficient computation through parallelization design, with a training delay of only 10 ms and a throughput of 2,900 samples/s (108 s faster than MODBNE). With a parameter size of 5.63 M, it occupied only 0.5 GB of memory, meeting real-time warning requirements. This may be due to the parallelization design of the model structure and GPU acceleration optimization, which enables it to meet real-time requirements while maintaining high accuracy. Other complex models such as DBN have low computational efficiency due to the layer by layer pre-training mechanism, while ELM, although the fastest, has difficulty meeting engineering requirements in terms of accuracy (Naskath et al., 2023; Hua et al., 2024).

Although the IMCN model performs well overall, its significant prediction bias on specific engines may be due to the engine experiencing atypical composite failure modes or extreme time-varying conditions. If the efficiency of the high-pressure compressor suddenly drops and the combustion chamber hot spots coexist, it may cause the sensor signal to exhibit conflicting characteristics that contradict the main degradation path in the training set, thereby misleading the model. Through visual analysis of the attention weights of the Transformer module in IMCN, it was found that the model failed to continuously focus on key sensors that indicate core performance degrada-

tion when dealing with these abnormal cases, and was instead disrupted by certain instantaneous fluctuations. This indicates that the new model's understanding of complex physical coupling effects still relies on the statistical laws of the training data, rather than explicit physical knowledge. When faced with fault interactions that are not fully covered by the training set, its generalization ability is severely challenged. The series connection of multi-channel convolution and Transformer encoder in IMCN achieves the complementarity of "local feature extraction global dependency modeling", enabling the model to simultaneously capture the short-term fluctuations and long-term degradation correlations of sensor signals, thereby improving prediction accuracy. The AVMD preprocessing in HNM effectively removes background noise through adaptive signal decomposition, enhancing the sensitivity of subsequent CNN BiGRU to weak fault features. The research results can provide high-precision RUL prediction capability and reliable basis for optimizing maintenance cycle, avoiding unplanned grounding. Although this study has achieved some results, there are still some shortcomings, such as only analyzing aircraft engines, and further exploration is needed for the analysis effects of other engines. Moreover, this study only analyzed a portion of the data, and further analysis is needed for the generalizability of other data and directions.

Funding

References

Azyus, A. F., Wijaya, S. K., & Naved, M. (2022). Determining RUL predictive maintenance on aircraft engines using GRU. *Journal of Mechanical, Civil and Industrial Engineering*, *3*(3), 79–84. https://doi.org/10.32996/jmcie.2022.3.3.10

Boujamza, A., & Elhaq, S. L. (2022). Attention-based LSTM for remaining useful life estimation of aircraft engines. *IFAC-PapersOnLine*, *55*(12), 450–455. https://doi.org/10.1016/j.ifacol.2022.07.353

Chen, Ch., Lu, N., Jiang, B., & Xing, Y. (2022). A data-driven approach for assessing aero-engine health status. *IFAC-PapersOnLine*, *55*(6), 737–742. https://doi.org/10.1016/j.ifacol.2022.07.215

Chen, W., Liu, Ch., Chen, Q., & Wu, P. (2023). Multi-scale memory-enhanced method for predicting the remaining useful life of aircraft engines. *Neural Computing and Applications*, *35*(3), 2225–2241. https://doi.org/10.1007/s00521-022-07378-z

de Pater, I., & Mitici, M. (2023). A mathematical framework for improved weight initialization of neural networks using Lagrange multipliers. *Neural Networks*, *166*(1), 579–594. https://doi.org/10.1016/j.neunet.2023.07.035

Deng, S., & Zhou, J. (2024). Prediction of remaining useful life of aero-engines based on CNN-LSTM-attention. *International Journal of Computational Intelligence Systems*, *17*(1), Article 232. https://doi.org/10.1007/s44196-024-00639-w

George, B., & Muthuveerappan, N. (2023). Life assessment of a high temperature probe designed for performance evaluation and health monitoring of an aero gas turbine engine. *International Journal of Turbo & Jet Engines*, *40*(2), 139–146. https://doi.org/10.1515/tjeng-2020-0037

Hua, Z., Yang, Q., Chen, J., Lan, T., Zhao, D., Dou, M., & Liang, B. (2024). Degradation prediction of PEMFC based on BiTCN-BiGRU-ELM fusion prognostic method. *International Journal of Hydrogen Energy*, *87*, 361–372. https://doi.org/10.1016/j.ijhydene.2024.08.502

Jianqiang, W., Gexue, R., Yonghui, Ch., Quan, Y., Runeng, Zh., Chunlan, Ch., & Wanyuan, D. (2024). Analysis and verification of vibration isolation performance of engine mount based on low-frequency approximation method. *Journal of Low Frequency Noise, Vibration and Active Control*, *43*(3), 1223–1243. https://doi.org/10.1177/14613484241229813

Jiang, X., Wang, J., Shen, Ch., Shi, J., Huang, W., Zhu, Z., & Wang, Q. (2021). An adaptive and efficient variational mode decomposition and its application for bearing fault diagnosis. *Structural Health Monitoring*, *20*(5), 2708–2725. https://doi.org/10.1177/1475921720970856

Kaba, A., Aygun, H., & Turan, O. (2022). Multi-dimensional energetic performance modeling of an aircraft engine with the aid of enhanced least–squares estimation based genetic algorithm method. *Journal of Thermal Analysis Calorimetry*, *147*(10), 5913–5935. https://doi.org/10.1007/s10973-021-10922-z

Koul, A. K., & Dainty, R. V. (2022). Fatigue fracture of aircraft engine compressor disks. *Journal of Failure Analysis and Prevention*, *22*(5), 1995–2004. https://doi.org/10.1007/s11668-022-01516-4

Lee, D., Kwon, H.-J., & Choi, K. (2024). Risk-based maintenance optimization of aircraft gas turbine engine component. *Proceedings of the Institution of Mechanical Engineers, Part O: Journal of Risk Reliability*, *238*(2), 429–445. https://doi.org/10.1177/1748006X221135907

Lee, Y., Park, J., & Lee, D. (2022). Inspection interval optimization of aircraft landing gear component based on risk assessment using equivalent initial flaw size distribution method. *Structural Health Monitoring*, *21*(4), 1396–1406. https://doi.org/10.1177/14759217211033625

Liu, X., Zhu, J., Luo, C., Xiong, L., & Pan, Q. (2022). Aero-engine health degradation estimation based on an underdetermined extended Kalman filter and convergence proof. *ISA Transactions*, *125*(1), 528–538. https://doi.org/10.1016/j.isatra.2021.06.040

Liu, Y., Mo, D., Nalianda, D., Li, Y., & Roumeliotis, I. (2022). Review of more electric engines for civil aircraft. *International Journal of Aeronautical and Space Sciences*, *23*, 784–793. https://doi.org/10.1007/s42405-022-00469-0

Mourer, A., & Lacaille, J. (2022). Detection and correction of equipment biases during engine tests. *Insight*, *64*(8), 459–464. https://doi.org/10.1784/insi.2022.64.8.459

Naskath, J., Sivakamasundari, G., & Begum, A. A. S. (2023). A study on different deep learning algorithms used in deep neural nets: MLP SOM and DBN. *Wireless Personal Communications*, *128*(4), 2913–2936. https://doi.org/10.1007/s11277-022-10079-4

Rath, N., Mishra, R. K., & Kushari, A. (2024). Aero engine health monitoring, diagnostics and prognostics for condition-based maintenance: An overview. *International Journal of Turbo & Jet-Engines*, *40*(s1), 279–292. https://doi.org/10.1515/tjj-2022-0020

Szrama, S., Szymański, G., & Mokrzan, D. (2025). Aircraft propulsion health status prognostics and prediction. *Advances in Science and Technology Research Journal*, *19*(5), 321–335. https://doi.org/10.12913/22998624/202232

Tang, D., Bi, F., Lin, J., Li, X., Yang, X., & Bi, X. (2022). Adaptive recursive variational mode decomposition for multiple engine faults detection. *IEEE Transactions on Instrumentation and Measurement*, *71*(1), 1–11. https://doi.org/10.1109/TIM.2022.3173646

Wahid, A., Yahya, M., Breslin, J. G., & Intizar, M. A. (2023). Self-attention transformer-based architecture for remaining useful life estimation of complex machines. *Procedia Computer Science*, *217*(1), 456–464. https://doi.org/10.1016/j.procs.2022.12.241

Wang, Y., Zhao, H., Cheng, W., Zhang, Y., & Jia, L., & Li, Y. (2025). Data-driven dynamic health index construction for diagnosis and prognosis of Engine Bleed Air system. *Aerospace Systems*, *8*(1), 149–161. https://doi.org/10.1007/s42401-024-00318-w

Xu, T., Han, G., Zhu, H., Taleb, T., & Peng, J. (2023). Multi-resolution LSTM-based prediction model for remaining useful life of aero-engine. *IEEE Transactions on Vehicular Technology*, *73*(2), 1931–1941. https://doi.org/10.1109/TVT.2023.3319377

Yang, Q., Tang, B., Li, Q., Liu, X., & Bao, L. (2023). Dual-frequency enhanced attention network for aircraft engine remaining useful life prediction. *ISA Transactions*, *141*(1), 167–183. https://doi.org/10.1016/j.isatra.2023.06.020

Zhang, Z., Cheng, J., Chen, P., Gao, S., Chen, X., & Zio, E. (2025). Leveraging working-condition-related features for enhanced cross-domain remaining useful life prediction of aircraft engines. *The Journal of Supercomputing*, *81*, Article 573. https://doi.org/10.1007/s11227-024-06889-x

Zhou, Z., Long, Z., Wang, R., Bai, M., Liu, J., & Yu, D. (2024). An aircraft engine remaining useful life prediction method based on predictive vector angle minimization and feature fusion gate improved transformer model. *Journal of Manufacturing Systems*, *76*, 567–584. https://doi.org/10.1016/j.jmsy.2024.08.025